Comparison of Different Braking Strategies to Improve the Energy Recovery of an Electric Vehicle based on Cascaded H-Bridge Inverter with Batteries

Gaël Pongnot, Clément Mayet, Denis Labrousse

Comparison of Different Braking Strategies to Improve the Energy Recovery of an Electric Vehicle based on Cascaded H-Bridge Inverter with Batteries

Gaël Pongnot
SATIE – UMR CNRS 8029
Université Paris-Saclay – ENS Paris-Saclay
Gif-sur-Yvette, France
gael.pongnot@ens-paris-saclay.fr

Clément Mayet
SATIE – UMR CNRS 8029
Le Cnam – ENS Paris-Saclay
Paris, France
clement.mayet@lecnam.net

Denis Labrousse
SATIE – UMR CNRS 8029
Le Cnam – ENS Paris-Saclay
Paris, France
denis.labrousse@ens-paris-saclay.fr

***Abstract*—This paper deals with the improvement of energy recovery in a battery electric vehicle (BEV) using a cascaded H-bridge inverter with integrated battery cells (CHB-IB). Different braking strategies are defined based on the power map of the overall traction system. These strategies are simulated on a specific driving cycle. The results are compared to select the best strategies in terms of energy consumption.**

***Index Terms*—electric vehicles, cascaded H-bridge inverter, battery system, simulation, control, braking energy management strategy, recovery of energy, Energetic Macroscopic Representation.**

I. Introduction

Battery electric vehicles (BEV) are one of the solutions being considered to reduce greenhouse gas emissions from the transportation sector and address climate change [1], [2]. Sufficient market penetration of BEV requires improvements in the range and cost of current BEV [3]. Increasing the energy density of batteries and improving the overall efficiency of the traction system are therefore sought. In this context, this paper follows two parallel axes of improvement: the use of an innovative battery subsystem based on a Cascaded H-Bridge inverter with Integrated Battery cells (CHB-IB) [4]–[6], and the development of an energy management strategy capable of increasing energy recovery during braking phases [7]–[10].

An innovative topology based on a CHB-IB has recently been proposed to replace the conventional traction system of BEV. It consists of a series connection of several H-bridge converters with integrated battery cells. They supply the electric traction machine with a nearest level control. Previous papers have already described this new topology and its control [11]–[13]. The CHB-IB aims to fulfill the roles of voltage source inverter (VSI), battery management system (BMS) and charger. Significant improvements are expected compared to conventional topologies. A previous study evaluated the efficiency of the new topology [13]. A loss map was determined in the torque-speed plane of the electric traction machine.

This paper has been achieved within IBIS project, funded by ADEME PIA.

The purpose of this paper is to study the braking management of a BEV equipped with CHB-IB technology. Therefore, the objective is to develop and evaluate several energy management strategies to improve the overall efficiency during brake energy recovery. Section II will present the generalities of the considered BEV, its model, control, and braking management. Section III will briefly present the topology of the electric drive and its energetic model. Then, section IV will focus on the development of different braking strategies. Finally, these strategies will be evaluated and compared in section V. The conclusion and perspectives will be drawn in section VI.

All models will be organized using the Energetic Macroscopic Representation (EMR) [14]. The EMR is a graphical tool to organize multi-scale and multi-physical models respecting the physical properties of the system, such as the principles of energy interaction and causality [14], [15]. In addition, the control structure of the system under study, including the identification of degrees of freedom allowing the application of energy management strategies, can be deduced from the EMR according to specific inversion rules.

II. General Model of the BEV

The vehicle studied is a small segment BEV. It has a mass of 1.6 t including passengers. The vehicle consists of an electric drive (ED), which is connected to the mechanical transmission (MT). The ED consists of a permanent magnet synchronous machine (PMSM) powered by the CHB-IB. The MT consists of a mechanical gearbox and differential, wheels (including mechanical brakes), and the chassis of the BEV (fig. 1).

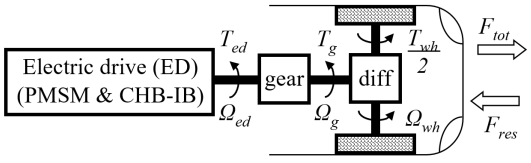

Fig. 1. Studied BEV

A. Model of the BEV

A simplified longitudinal model of the BEV is used in this subsection. The assumption of straight motion is considered, *i.e.*, no curves are considered and, thus, the torques of the wheels (right and left) can be considered as perfectly equal. At the vehicle level, the EMR is shown in fig. 2. Three energy sources (green oval pictograms) represent the ED, the mechanical brake, and the environment, respectively. The MT is modeled and represented by several different EMR elements. All elements and sources are detailed below.

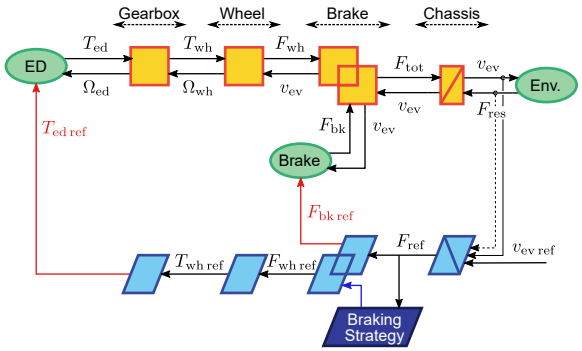

Fig. 2. EMR of the studied BEV

The environment is a source that imposes the resistive force F_{res} on the movement of the vehicle (1). It depends on the rolling resistance F_{roll} and the aerodynamic resistance F_{aero}, depending on the longitudinal speed of the BEV v_{ev}.

$$F_{\text{res}} = F_{\text{roll}} + F_{\text{aero}}(v_{\text{ev}}) \tag{1}$$

The vehicle speed v_{ev} is calculated using the Newton's Law (2), with M_{ev} the total mass of the vehicle and F_{tot} the total traction/braking force applied by the vehicle on the chassis. It is represented by an accumulation element.

$$v_{\text{ev}} = \frac{1}{M_{\text{ev}}} \int (F_{\text{tot}} - F_{\text{res}})\, \mathrm{d}t \tag{2}$$

The force F_{tot} is the sum of the wheel force F_{wh} and the mechanical brake force F_{bk} (3). A coupling element is used.

$$F_{\text{tot}} = F_{\text{wh}} + F_{\text{bk}} \tag{3}$$

An equivalent mechanical brake is represented by a source, which imposes the mechanical braking force F_{bk} equal to its reference $F_{\text{bk\,ref}}$, determined by the control of the BEV.

An equivalent wheel is considered according to the straight motion assumption. It is represented by a conversion element with equation (4), where r_{wh} is the wheel radius, T_{wh} is the torque applied on the equivalent wheel, and Ω_{wh} its rotational speed.

$$\begin{cases} F_{\text{wh}} = T_{\text{wh}}/r_{\text{wh}} \\ \Omega_{\text{wh}} = v_{\text{ev}}/r_{\text{wh}} \end{cases} \tag{4}$$

The gearbox and differential are then represented by another conversion element. The model is described by (5), with T_{ed} the electromechanical torque and Ω_{ed} the rotational speed of the drive, and with k_g the reduction ratio and η_g the efficiency.

$$\begin{cases} T_{\text{wh}} = T_{\text{ed}} k_g \eta_g^{\text{sign}(T_{\text{ed}}\Omega_{\text{ed}})} \\ \Omega_{\text{ed}} = k_g \Omega_{\text{wh}} \end{cases} \tag{5}$$

Finally, the ED is a reversible source of torque T_{ed}, which is controlled via the control variable $T_{\text{ed\,ref}}$. At the vehicle level, it is assumed that $T_{\text{ed}} = T_{\text{ed\,ref}}$. This source includes the PMSM and CHB-IB models, as well as the torque control. It requires the rotational speed of the drive as an input Ω_{ed}. The objective of the ED model is to estimate the energy consumed in the cells of the battery, considering the various losses. It will be further detailed in Section III. A control is required to define the 2 tuning variables, namely the references of the force of the mechanical brake $F_{\text{bk\,ref}}$ and of the torque of the ED $T_{\text{ed\,ref}}$. The control is explained in the next subsection.

B. Control of the BEV

A control (light blue elements) is deduced from the EMR using inversion rules. The objective is to control the velocity of the BEV by correctly determining the two available tuning variables. A tuning path is thus deduced to link the objective variable to the tuning variables. All EMR elements present on this path are inverted. Accumulation elements are indirectly inverted (closed loop control), while coupling and conversion elements are directly inverted.

The accumulation element (2) is inversed indirectly by a velocity controller $C(s)$ (with s the Laplace variable). The objective is to track the velocity reference $v_{\text{ev\,ref}}$ according to the velocity measurement v_{ev} and the rejection of the resistive force measurement F_{res}, which is a disturbance (6). The output of this operation defines the total traction/braking force $F_{\text{tot\,ref}}$ to be produced by the BEV.

$$F_{\text{tot\,ref}} = F_{\text{res}} + C(s)\,(v_{\text{ev\,ref}} - v_{\text{ev}}) \tag{6}$$

Then, the coupling element (3) is inverted by (7). It is used to distribute the total reference traction/braking force between the wheel force $F_{\text{wh\,ref}}$ and mechanical brake force $F_{\text{bk\,ref}}$ references, especially during the braking phase. This allows the application of recovery braking energy management strategies by imposing the reference wheel force. During the braking, the brake is used to compensate the missing braking force. Of course, during the traction phase, the brake must be inhibited. The braking management strategy problem is introduced in the next subsection and will be more detailed in Section IV.

$$F_{\text{bk\,ref}} = F_{\text{tot\,ref}} - F_{\text{wh\,ref}} \tag{7}$$

Finally, the wheels (4) and gearbox and differential (5) are directly inversed to give the electric drive reference torque.

$$T_{\text{wh\,ref}} = r_{\text{wh\,ref}} F_{\text{wh\,ref}} \tag{8}$$

$$T_{\text{ed\,ref}} = T_{\text{wh\,ref}}/k_g \tag{9}$$

C. Recovery braking energy management of the BEV

Energy management must be developed to improve the recovery of braking energy and thus maximize battery recharging and reduce overall vehicle consumption, during the operating cycle. The role is therefore to define when the braking energy should be recovered by the ED or dissipated in the mechanical brake, and in what proportion. Of course, during the traction phase, the brake is inhibited, so $F_{\text{wh ref}} = F_{\text{tot ref}}$. However, during the braking phase, different strategies can be applied [7]. This is achieved by applying a certain recoverable braking force on the wheel $F_{\text{wh ref}}$, negative sign during braking, which will induce a specific braking torque on the ED $T_{\text{ed ref}}$.

The ED, being reversible, is therefore able to recover braking energy to the battery cells. However, the various constraints of the system must be respected, such as the torque and power limits of the ED and the state of charge (SoC) of the battery. The state of charge constraint will not be studied in this paper. Furthermore, the losses generated within the system during energy recovery must be considered in order not to produce unexpected additional losses, which could be higher than the recoverable energy. For this reason, and contrary to what would seem obvious, it is important to limit the possible (recoverable) braking force $F_{\text{lim rec}}$ according to these criteria, depending on the speed of the BEV (10).

$$F_{\text{wh ref}} = \max\left(F_{\text{tot ref}}, F_{\text{lim rec}}\right) \tag{10}$$

As an illustration, fig. 3 represents a driving cycle and the corresponding operating points in the torque-speed plane of the ED, in the case where braking is only regenerative (no activation of the mechanical brake). The objective of the braking energy management will therefore be to limit the torque, for negative power operating points (braking), to improve the consumption.

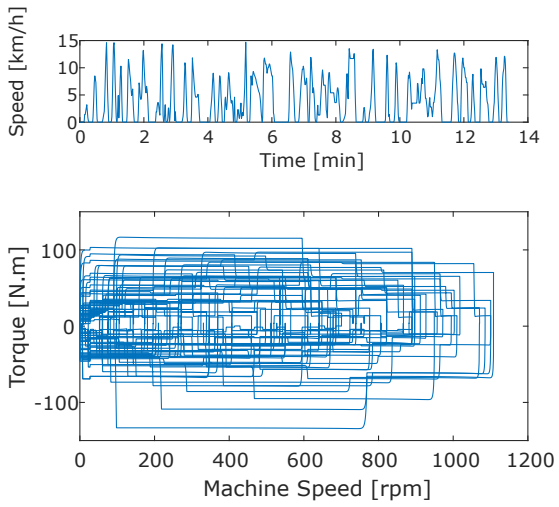

Fig. 3. Drive cycle and operating points in the torque-speed plane of the ED

III. Model of the ED

The topology of the ED is presented in fig. 4. As previously mentioned, it consists of several H-bridge converters with integrated battery (CHB-IB) connected in series for each phase of the system. The CHB-IB is controlled to supply the PMSM and finally to control the torque produced by the ED T_{ed}. The detailed model and control of the CHB-IB associated with the PMSM has already been presented in [11]–[13].

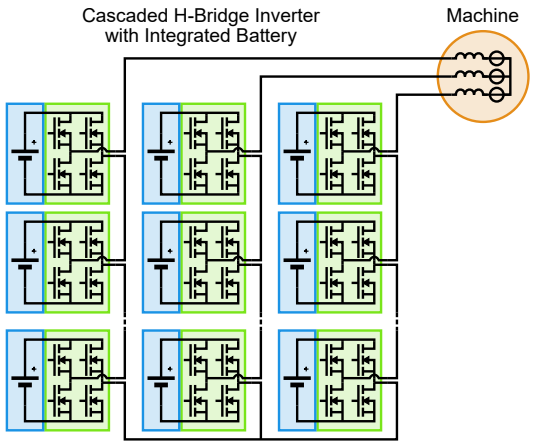

Fig. 4. Studied ED

A. Detailled model of the CHB-IB-based traction system

In [11]–[13], the EMR methodology was used to model, represent, and control the ED in detail. The losses were accurately modeled and took into account the internal losses of the battery, conduction and switching losses of the power electronic components, as well as the joule and iron losses of the machine.

In addition, the complete torque control of the ED was developed and presented. As can be seen in [13], the ED model and control relates the mechanical power of the ED (actual and reference torque and speed) to the chemical power (and thus stored chemical energy) of the battery.

This model allows for the simulation of different operating points where the actual rotation speed of the ED Ω_{ed}, the reference torque of the ED $T_{\text{ed ref}}$, and initial SoC of the battery are imposed. The results yield the actual chemical power that charges or discharges the battery cells according to the losses, control, and strategy of the ED.

B. Power map of the CHB-IB-based traction system

The detailed model has been used to derive a power map, which provides the chemical power recovered or supplied by the battery (in charge and in discharge) in a torque/speed plane (fig. 5) [13]. It can be observed that when the torque is negative (braking phase), the chemical power is mostly negative, which means that the battery cells are recharged, which is the normal expected behavior.

However, in some specific areas, the chemical power is positive although the BEV is braking. This means that the losses in the ED are greater than the recoverable braking

energy. Therefore, the ED requires the battery to consume energy to maintain the expected operating point, *i.e.*, the vehicle consumes battery energy to brake. These specific operating cases are absurd and should be avoided to improve overall energy consumption. Based on this map, the objective is therefore to propose an improved braking strategy that considers these specific operating points.

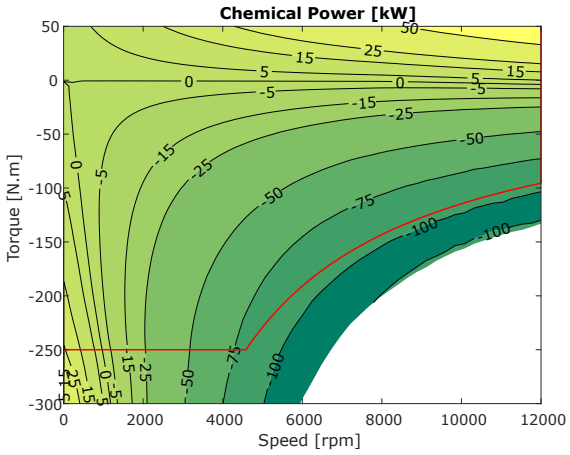

Fig. 5. Chemical power map of the ED

IV. Breaking Energy Management Strategies

In this section, and based of the observation from the previous section, 4 different braking strategies are proposed and described (fig. 6). They will be compared in Section V.

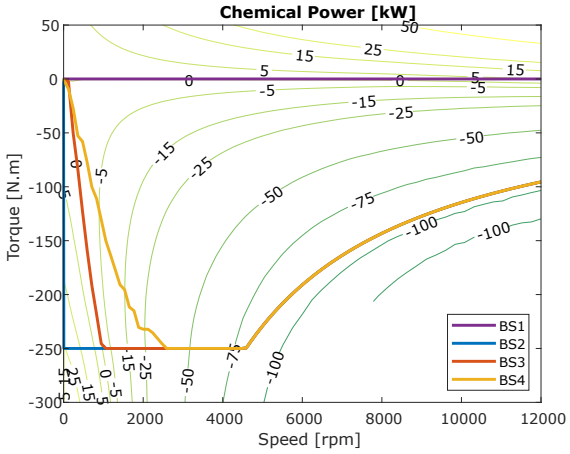

Fig. 6. Differents braking energy strategies considered

A. Braking Strategy 1 (BS1)

For reference, the first braking strategy consists in not recovering any energy. All braking energy is dissipated in the mechanical brake. Thus, the limit of the possible braking recovery force $F_{\text{lim rec}}$ is simply set to zero (11). It corresponds to the purple line in fig. 6.

$$F_{\text{lim rec}}(v_{\text{ev}}) = 0 \tag{11}$$

B. Braking Strategy 2 (BS2)

The second braking strategy is to recover all the braking energy as long as the braking power $P_{\text{ed max}}$ and braking torque $T_{\text{ed max}}$ limits of the ED are met. A torque limit $T_{\text{ed lim}}$ is determined in (12) depending on the rotation speed Ω_{ed} and the above limits. Since the braking energy management is applied to the linear variables of the BEV (force and linear speed), the torque limit is converted from (4) and (5) to a force limit that depends on v_{ev} (13). This limit is finally applied to the braking energy management (7). It corresponds to the blue line in fig. 6.

$$T_{\text{ed lim}}(\Omega_{\text{ed}}) = -\min\left(T_{\text{ed max}}, \frac{P_{\text{ed max}}}{\Omega_{\text{ed}}}\right) \tag{12}$$

$$F_{\text{lim rec}}(v_{\text{ed}}) = \frac{k_g}{r_{wh}\eta_g} T_{\text{ed lim}}\left(k_g \frac{v_{\text{ev}}}{r_{\text{wh}}}\right) \tag{13}$$

C. Braking Strategy 3 (BS3)

The third braking strategy considers the same limitations as the second strategy (14). However, it also takes into account the chemical power map of the ED, where areas with positive chemical power during braking are completely prohibited.

A boundary line can be drawn to distinguish between positive and negative chemical power areas in the map (fig. 6). This line can be expressed as a new torque limit $T_{\text{ed lim}}(\Omega_{ed})$, as a function of the speed of the ED. This torque $T_{\text{ed lim}}(\Omega_{ed})$ is expressed in (14) as the result of a minimisation of the torque T_{ed} with respect to the machine limits. This torque limit is also derived into a force limit using (13), from (4) and (5). It corresponds to the red line in fig. 6.

$$T_{\text{ed lim}}(\Omega_{ed}) = \operatorname{argmin} T_{\text{ed}} \quad \text{with} \begin{cases} T_{\text{ed lim}}(\Omega_{\text{ed}}) \geq -\min\left(T_{\text{ed max}}, \frac{P_{\text{ed max}}}{\Omega_{\text{ed}}}\right) \\ P_{\text{chem}}(\Omega_{\text{ed}}, T_{\text{ed}}) \leq 0 \end{cases} \tag{14}$$

D. Braking Strategy 4 (BS4)

The third strategy avoids consuming battery energy during braking by prohibiting certain nonsense operating points. However, when the operating points are limited by the boundary line (fig. 6), the chemical power of the battery is zero, which means that the PMSM is used in recovery mode, but no energy is actually stored in the battery due to losses.

Therefore, the fourth strategy aims to improve energy recovery by finding a maximum regenerated power line (MRPL) on the chemical power map. Indeed, in some specific operations, it is observed that reducing the braking torque of the ED results in more regenerated energy in the battery. Mechanical brakes compensate for torque difference.

The MRPL results in a new torque limitation $T_{\text{ed lim}}(\Omega_{ed})$, which also depends on the rotation speed of the ED. The torque limit is written as a minimisation of the chemical power according to the machine limits (15). It corresponds to the yellow line in fig. 6.

$$T_{\text{ed lim}}(\Omega_{ed}) = \text{argmin } P_{\text{chem}}(\Omega_{\text{ed}}, T_{\text{ed}})$$
$$\text{with } T_{\text{ed lim}}(\Omega_{\text{ed}}) \geq -\min\left(T_{\text{ed max}}, \frac{P_{\text{ed max}}}{\Omega_{\text{ed}}}\right) \quad (15)$$

V. Simulation Results and Comparisons

The simulations are performed on the driving cycle presented in fig. 3 with the 4 strategies (see fig. 6). Figure 7 shows the torque as a function of time over the whole driving cycle. It can be observed that the positive torques are the same for all strategies, which is normal since the strategies only act during braking. However, during braking, some of the operating points of the ED are different.

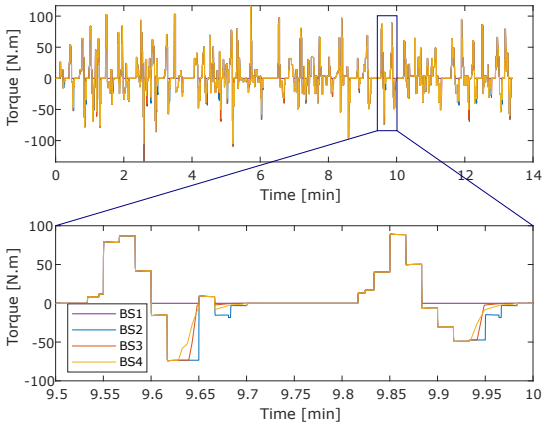

Fig. 7. Torque over time for the different strategies

This can also be observed by plotting the operating points on the chemical power map in the speed/torque plane for all strategies (fig. 8). Depending on the different strategies, some of the regenerative braking points are limited by the different torque limiting curves from fig. 6.

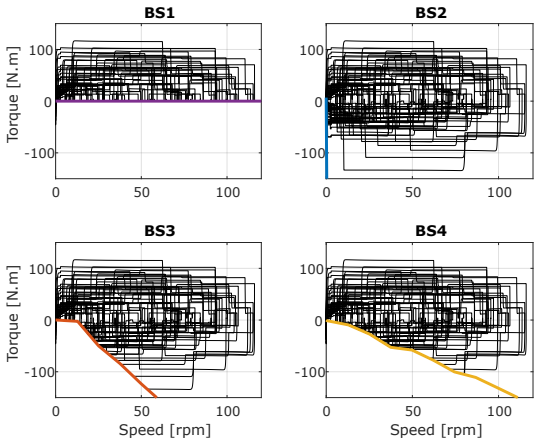

Fig. 8. Operating points in the torque/speed plane

Finally, the amount of chemical energy consumed in the battery cells as a function of time is presented in fig. 9. The results obtained with strategy 1 (no regenerative braking) show that 181 Wh of chemical energy are required during traction. This amount is reduced to 143 Wh with strategy 2, 136 Wh with strategy 3, and even 135 Wh with strategy 4.

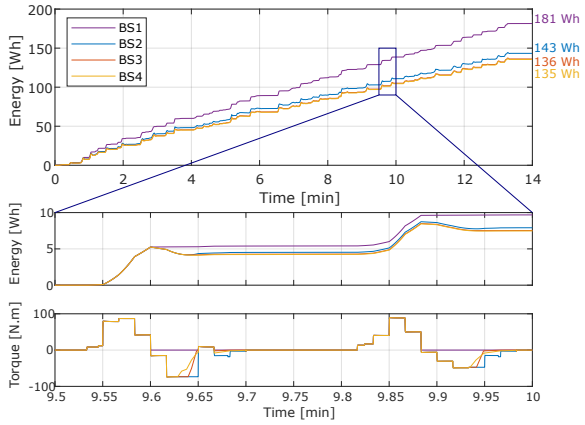

Fig. 9. Chemical energy consumption in the battery cells

The first braking strategy is a worst case reference. The introduction of a naive regenerative mode with BS2 recovers 38 Wh, a 21% reduction in consumption. However, this braking strategy consumes energy from the batteries for some operating points, like at 9.65 min where fig. 9 show an increase in energy for BS2 whereas the mecanical power is still negative. This is the consequence of the positive chemical power area in fig. 5 since mechanical power is negative, located at low speed. Then, BS3 avoid this area by considering only negative chemical power for recovery mode, this gives 5% reduction in consumption compared to BS2. An optimal braking strategy is found by using BS4, by choosing the limit torque to maximise the chemical energy recovery. Nevertheless, the different between BS3 and BS4 is less than 1%.

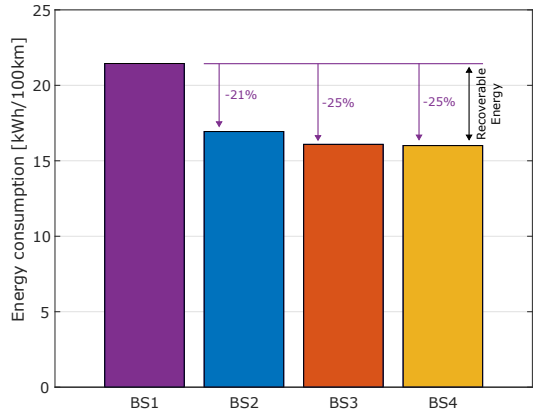

Fig. 10. Energy consumption for the different strategies

In the end, this means that 25% of the total energy consumed can be saved by using an appropriate braking energy

management strategy. The other conclusion that can be drawn from these results is that 17% of the potentially recoverable energy can be lost in the system during braking if the system losses are not properly considered. Of course, these figures may vary from one driving cycle to another and for different SoC values and temperature. However, understanding the BEV losses during braking is critical to improving overall energy consumption by applying the correct braking strategy.

VI. Conclusion

This paper compares different braking energy management strategies of a battery electric vehicle (BEV) based on cascaded H-bridged converters with integrated batteries (CHB-IB), which supplies a permanent magnet synchronous machine. The system losses are considered to improve the braking strategy to increase the regenerated energy in the battery cells and thus reduce the overall energy consumption. The simulation results show that 25% of the traction energy can be saved by applying an appropriate braking strategy. The results also show that a good knowledge of the losses in the BEV power train during braking is essential to improve the overall energy consumption by applying the right braking strategy. Indeed, taking into account the losses in the braking strategy can improve the energy consumption by 6% over the studied BEV and driving cycle.

However, these results depend on the chosen driving cycle and on battery conditions : SoC and temperature. Further studies will need to find the sensibility of the braking strategy to these parameters. Moreover, complex braking strategies, such as BS3 and BS4, needs an accurate behaviour model of the traction chain. Other studies could think about the feasibility and the cost-benefit analysis of such strategies.

References

[1] M. Ehsani, Y. Gao, S. Longo, and K. M. Ebrahimi, *Modern Electric, Hybrid Electric, and Fuel Cell Vehicles*, 3rd ed. Boca Raton: CRC Press, Mar. 2, 2018, 572 pp.

[2] C. C. Chan, "The State of the Art of Electric, Hybrid, and Fuel Cell Vehicles," *Proceedings of the IEEE*, vol. 95, no. 4, pp. 704–718, Apr. 2007.

[3] L. Paoli, A. Dasgupta, and S. McBain, "Electric Vehicles," IEA, Paris, 2022.

[4] M. Quraan, T. Yeo, and P. Tricoli, "Design and Control of Modular Multilevel Converters for Battery Electric Vehicles," *IEEE Transactions on Power Electronics*, vol. 31, no. 1, pp. 507–517, Jan. 2016.

[5] F. Chang, O. Ilina, M. Lienkamp, and L. Voss, "Improving the Overall Efficiency of Automotive Inverters Using a Multilevel Converter Composed of Low Voltage Si mosfets," *IEEE Transactions on Power Electronics*, vol. 34, no. 4, pp. 3586–3602, Apr. 2019.

[6] O. Theliander, A. Kersten, M. Kuder, W. Han, E. A. Grunditz, and T. Thiringer, "Battery Modeling and Parameter Extraction for Drive Cycle Loss Evaluation of a Modular Battery System for Vehicles Based on a Cascaded H-Bridge Multilevel Inverter," *IEEE Transactions on Industry Applications*, vol. 56, no. 6, pp. 6968–6977, Nov. 2020.

[7] A. S. Murthy, D. P. Magee, and D. G. Taylor, "Vehicle braking strategies based on regenerative braking boundaries of electric machines," in *2015 IEEE Transportation Electrification Conference and Expo (ITEC)*, Jun. 2015, pp. 1–6.

[8] W. Xu, H. Chen, J. Wang, and H. Zhao, "Velocity Optimization for Braking Energy Management of In-Wheel Motor Electric Vehicles," *IEEE Access*, vol. 7, pp. 66 410–66 422, 2019.

[9] W. Li, H. Du, and W. Li, "Four-Wheel Electric Braking System Configuration With New Braking Torque Distribution Strategy for Improving Energy Recovery Efficiency," *IEEE Transactions on Intelligent Transportation Systems*, vol. 21, no. 1, pp. 87–103, Jan. 2020.

[10] S. Heydari, P. Fajri, R. Sabzehgar, and A. Asrari, "Optimal Brake Allocation in Electric Vehicles for Maximizing Energy Harvesting During Braking," *IEEE Transactions on Energy Conversion*, vol. 35, no. 4, pp. 1806–1814, Dec. 2020.

[11] C. Mayet, D. Labrousse, R. Bkekri, F. Roy, and G. Pongnot, "Energetic Macroscopic Representation and Inversion-Based Control of a Multi-Level Inverter with Integrated Battery for Electric Vehicles," in *2021 IEEE Vehicle Power and Propulsion Conference (VPPC)*, Gijon, Spain: IEEE, Oct. 2021, pp. 1–6.

[12] G. Pongnot, C. Mayet, and D. Labrousse, "Modeling and Estimation of the Losses of a Multi-Level Inverter with Integrated Battery for Electric Vehicles," in *PCIM Europe 2022*, Nuremberg, Germany, May 2022.

[13] G. Pongnot, C. Mayet, and D. Labrousse, "Loss distribution in an Electric Vehicle Traction Chain using a Cascaded H-Bridge Inverter with Integrated Battery," in *PCIM Europe 2023*, Nuremberg, Germany, May 2023.

[14] A. Bouscayrol, J.-P. Hautier, and B. Lemaire-Semail, "Graphic Formalisms for the Control of Multi-Physical Energetic Systems: COG and EMR," in *Systemic Design Methodologies for Electrical Energy Systems*, John Wiley & Sons, Ltd, 2012, pp. 89–124.

[15] Y. Iwasaki and H. A. Simon, "Causality and model abstraction," *Artificial Intelligence*, vol. 67, no. 1, pp. 143–194, May 1, 1994.